Research article

Estimation of the expected number of cases of microcephaly in Brazil as a result of Zika

Yanfeng Liang*and **David Greenhalgh**

Department of Mathematics and Statistics, University of Strathclyde, Glasgow, G1 1XH, UK

* **Correspondence:** Email: yanfeng.liang@hotmail.com.

Abstract: In this paper we have adapted a delayed dengue model to Zika. By assuming that the epidemic starts by a single infected individual entering a disease-free population at some initial time t_0 we have used the least squares parameter estimation technique in R to estimate the initial time t_0 using observed Zika data from Brazil as well as the transmission probabilities of Zika in Brazil between humans and mosquitoes and vice-versa. Different values of *Aedes aegypti* (*A. aegypti*) biting rate are used throughout the paper.

We have estimated the value of the basic reproduction number for Zika in Brazil and calculated the expected number of cases of microcephaly in newborns as a result of women infected with Zika during pregnancy. We started off with a non-age-structured model then introduced age-structure into the model.

However in reality seasonality, in particular temperature and rainfall, have a great impact on the population size of *A. aegypti*. Hence we repeat both the non-age-structured and age-structured analyses introducing seasonality into the *A. aegypti* birth function to model the effect of these environmental factors.

Keywords: Zika virus; microcephaly; dengue; *Aedes aegypti*; parameter estimation; least square estimation; ordinary differential equations; partial differential equations

1. Introduction

The Zika virus is spread by the same species of mosquito, *namely Aedes aegypti* (*A. aegypti*), as dengue. It is a member of the virus family *Flaviviridae*. The first discovery of the Zika virus was in 1947, however despite being around for a while, the Zika virus has not received much attention until recently when it has been discovered that it is associated with microcephaly which is a serious birth defect in newborns, caused if women are infected with Zika during pregnancy. Most importantly there is still no vaccine to prevent the Zika virus. Apart from causing severe birth defects to newborn

babies, infected individuals can also experience fever, rash and joint pain. As a result, in this paper we will use an existing mathematical model for dengue to analyse the dynamical behaviour for the Zika virus, especially in Brazil, as well as obtaining the future expected number of cases of microcephaly due to Zika. Although the Zika virus and dengue are very similar and thus some parameter values would remain the same, parameters such as the transmission probabilities as well as the basic reproduction number may vary. Therefore in this paper we will also use some existing data values in Brazil to estimate those required parameter values. We will use four different approaches to estimate the expected number of cases of microcephaly in Brazil due to pregnant women exposed to the Zika virus.

This paper is arranged as follows: In Section 2, we will look at the first approach by working with a delayed dengue model without seasonality as well as defining the parameter values. We will then look at the results obtained by using the least squares estimation technique in R. The basic reproduction number for our model without seasonality is also calculated. In Section 3, we will look at the second approach where we will improve on our model by adding seasonality into the birth function of the *A. aegypti* mosquitoes. In Section 4, we will continue to work with the same model as in Section 2, but we will make the model more realistic, but also more complicated, by taking into account the age-structure of the human population. In Section 5, we will look at the last approach where we introduce seasonality into the more complicated age-structured model given in Section 4. Lastly in Section 6, we will summarise all our results. Numerical simulations are produced throughout the paper to illustrate our findings.

2. The delayed Zika model without seasonality

Let us define $S_H(t)$, $I_H(t)$ and $R_H(t)$ to respectively represent the susceptible, infected and recovered individuals for humans, while $S_v(t)$, $L_v(t)$ and $I_v(t)$ respectively represent the susceptible, latent and infected mosquitoes. $N_H = S_H + I_H + R_H$ denotes the total human population size and $N_v = S_v + L_v + I_v$ represents the total *A. aegypti* population size where both populations are constant. The delayed mathematical model for dengue mentioned in [1] is as follows:

$$\frac{dS_H(t)}{dt} = -abI_v(t)\frac{S_H(t)}{N_H} - \mu_H S_H(t) + \mu_H N_H,$$

$$\frac{dI_H(t)}{dt} = abI_v(t)\frac{S_H(t)}{N_H} - (\mu_H + \gamma)I_H(t),$$

$$\frac{dR_H(t)}{dt} = \gamma I_H(t) - \mu_H R_H(t),$$

$$\frac{dS_v(t)}{dt} = -acS_v(t)\frac{I_H(t)}{N_H} - \mu_v S_v(t) + \mu_v N_v,$$

$$\frac{dL_v(t)}{dt} = acS_v(t)\frac{I_H(t)}{N_H} - \mu_v L_v(t) - acS_v(t-\tau)\frac{I_H(t-\tau)}{N_H}e^{-\mu_v \tau},$$

$$\frac{dI_v(t)}{dt} = acS_v(t-\tau)\frac{I_H(t-\tau)}{N_H}e^{-\mu_v \tau} - \mu_v I_v(t),$$

with initial conditions $S_H(t_0), R_H(t_0), I_v(t_0), L_v(t_0), \{I_H(\eta) : \eta \in [t_0 - \tau, t_0]\}$ and $\{S_v(\eta) : \eta \in [t_0 - \tau, t_0]\}$. The definitions of the parameter values used in Eq (2.1) and their corresponding values are given in Table 1.

Note that the model described by Eq (2.1) does not have an exposed class in humans. However, it is important to note that much work has already been done on the Zika virus without a human exposed class [2–12]. Therefore, we hope that the results mentioned in this paper will be able to contribute to this research area.

Table 1. Parameter values given in Eq (2.1).

Parameter values	Biological meanings	Values
a	*A. aegypti* biting rate	Variable
b	Probability of transmission of Zika when an infectious mosquito bites a susceptible human	$0.10 - 0.75$ [14]
c	Probability of transmission of Zika when a susceptible mosquito bites an infectious human	$0.30 - 0.75$ [15]
N_H	Human population in Brazil in 2015	$207,848,000$ [16]
μ_H	Per capita human mortality rate in Brazil	$1/(75 \times 52)$/week [16]
γ	Per capita human recovery rate	$7/6$/week [13]
μ_v	Per capita mortality rate for *A. aegypti*	0.025×7/week [1]
N_v	*A. aegypti* population	$1.5 \times N_H$ [17, 18]
τ	Zika extrinsic incubation period	$8.2/7$ weeks [13]

As we can see from Table 1, the two most crucial parameter values b and c can take values within the ranges given and thus one of the main aims in this project is to use the least squares estimation technique in R and the real Zika virus data (the weekly incidence cases of Zika) from Brazil given in [13] to estimate these two parameter values. In the next section, we will discuss in detail the idea behind the estimation technique.

2.1. Parameter estimation

The basic reproduction number is defined as the expected number of secondary cases caused when a newly infected individual enters a disease-free population at equilibrium. A secondary case is a case infected from the original infected case via only one mosquito. In the context of mosquito-borne disease such as Zika it can equally be defined as the expected number of secondary cases caused when a newly infected mosquito enters a disease-free population at equilibrium. All epidemics begin with a single infected host entering a disease-free population and the basic reproduction number R_0 exceeds one. Therefore in our case, it is reasonable to assume that a single Zika infected human enters the disease-free population at some time t_0, where $t_0 < t_1$ and t_1 is the time when we have available Zika data values in Brazil obtained from [13]. In this case t_1 represents the first week in 2015. Let us now assume a single infected human has entered the Brazilian population at some time before t_1, say t_0, where $S_H(t_0) = 207,847,999$, $I_H(t_0) = 1$, $R_H(t_0) = 0$, $L_v(t_0) = 0$, $I_v(t_0) = 0$, $\{I_H(\eta) = 0$ for $\eta \in [t_0 - \tau, t_0]\}$ and $\{S_v(\eta) = 207,848,000 \times 1.5$ for $\eta \in [t_0 - \tau, t_0]\}$. Note that these initial values correspond to the time t_0 at which the first human case of Zika virus was first introduced into a disease-free population. The values of these variables at the later time t_1 will be different.

Table 2. Estimated values for b, c and $t_1 - t_0$ for different biting rates to 4 decimal places (d.p.) $t_1 - t_0$ is measured in weeks.

| A. *aegypti* biting rate per day	b	c	$t_1 - t_0$
0.20	0.2489	0.4513	180.5848
0.50	0.45	0.75	500

Table 3. 95% confidence interval for the estimated values given in Table 2 to 4 d.p.

| A. *aegypti* biting rate per day	b	c	$t_1 - t_0$
0.20	(0.2477, 0.2502)	(0.4397, 0.4628)	(173.1913, 187.9783)
0.50	(0.4485, 0.4515)	(0.7462, 0.7538)	(496.0399, 503.9601)

We used the least squares estimation technique in R (R version 3.0.2, Frisbee Sailing 2013 version) using the function `nls.lm` and the library `minpack.lm` to perform the least squares fitting. By comparing the least square minimised results with the real data values for Zika cases in Brazil given in [13], the estimated values for b, c and $t_1 - t_0$ with different values of a are given in Table 2 where $t_1 - t_0$ is in units of weeks. The corresponding 95% confidence intervals for the estimated values are given in Table 3. Clearly, all the values we obtained for both b and c lie within the appropriate ranges mentioned by Andraud et al. [14] and Chikak and Ishikama [15].

Note that in Eq (2.1) if we multiply a by a constant factor k, divide both b and c by the same factor, and keep t_0 the same, then the output of the model does not change. Therefore, when we had found the optimal least squares fitted values b and c corresponding to $a = 0.20$ per day, we could then find the optimal values of b and c for the other values of a by dividing those values for $a = 0.20$ per day by the appropriate factor and keeping t_0 the same. As a result, we have chosen to illustrate only the results obtained for when $a = 0.20$ per day.

Note also that applying the procedure suggested above to $a = 0.50$ per day (namely dividing b and c from $a = 0.20$ per day by a factor of 2.5) gives resulting values of b and c which are outside the constraints for these model parameters suggested by the literature. As a result, we have decided to obtain an alternative set of optimal values for when $a = 0.50$ per day, where b and c are within the ranges suggested by literature. In this situation, these constraints force the least squares algorithm to fit to a later phase of the epidemic after most people have become infected (note the number of recovered humans in expressions (2.1) and (2.2)). Hence the model predictions with the least squares fitted parameters are virtually the same for $a = 0.20$ per day, $a = 0.25$ per day and $a = 0.30$ per day but different for $a = 0.50$ per day.
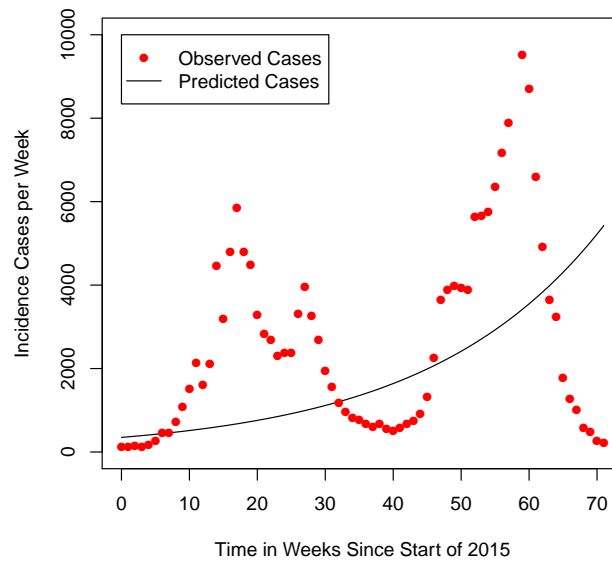
Figure 1. Numerical simulation for predicted cases for Zika obtained from Eq (2.1) plotted against the real data from Brazil from [13] with the unit of time in weeks, starting from the beginning of 2015 where $a = 0.20$/day.
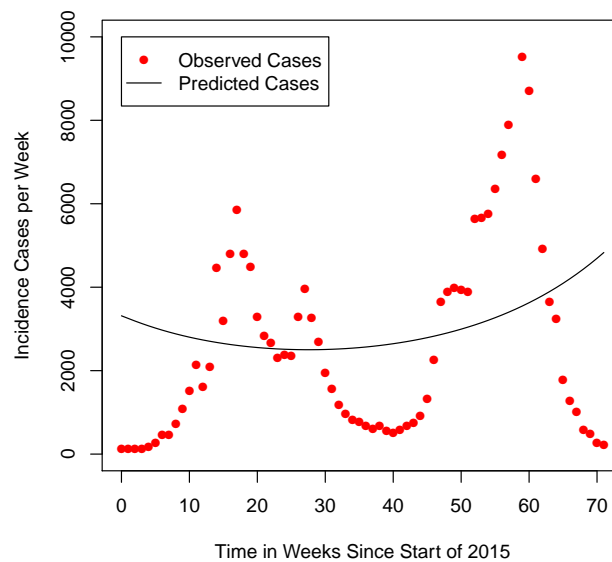
Figure 2. Numerical simulation for predicted cases for Zika obtained from Eq (2.1) plotted against the real data from Brazil from [13] with the unit of time in weeks, starting from the beginning of 2015 where $a = 0.50$/day.

For the purpose of illustration, the data fitting against the real Zika data using Eq (2.1) for $a = 0.20$/day and $a = 0.50$/day are given in Figure 1 and Figure 2 respectively. The results shown in these figures are not a perfect fit and one of the main reasons could be that seasonality is not included in Eq (2.1). Motivated by this, later on in this paper, we will modify Eq (2.1) by including seasonality into the model to improve the data fitting and the accuracy of our estimation.

In addition, in order to allow us to make more estimates for the future expected number of cases of microcephaly, it is important that we have reasonable starting values for S_H, I_H, R_H, S_v, L_v and I_v. As a result, by keeping the assumption that a single infected human enters a disease-free population at some point t_0, we also obtained estimated expected values at time t_1 corresponding to different biting rates given as follows. In each case the values of $S_v(\eta)$ and $I_H(\eta)$ for $\eta \in [t_1 - \tau, t_1]$ are given by the simulation using the estimated parameters.

- For $a = 0.20$/day and $t_1 = t_0 + 180.5848$ weeks, the values at time t_1 are

$$
\begin{aligned}
S_H(t_1) &= 207,838,200, I_H(t_1) = 314.4883, R_H(t_1) = 9,470.184, \\
S_v(t_1) &= 311,770,600, L_v(t_1) = 308.5773, I_v(t_1) = 1,087.741.
\end{aligned}
\tag{2.1}
$$

- For $a = 0.50$/day and $t_1 = t_0 + 500$ weeks, the values at time t_1 are

$$
\begin{aligned}
S_H(t_1) &= 6,780,497, I_H(t_1) = 2,868.188, R_H(t_1) = 201,064,600, \\
S_v(t_1) &= 311,695,900, L_v(t_1) = 12,090.84, I_v(t_1) = 63,965.19.
\end{aligned}
\tag{2.2}
$$

The values at time t_1 will be used as initial values for future simulations in Section 2.3.

Now that we have all the required parameter values and the initial values for each biting rate, we can estimate the future expected number of cases of microcephaly as a result of pregnant women infected with Zika during pregnancy. However before we do this, it is important for us to find another important epidemiological parameter value namely the basic reproduction number.

2.2. The basic reproduction number

The basic reproduction number, R_0, is a very important parameter value in infectious disease modelling as it often acts as a threshold which determines whether a particular epidemic will die out ($R_0 < 1$) or persist ($R_0 > 1$). In the context of our model the basic reproduction number is defined as the expected number of secondary cases of disease caused by a single newly infected individual entering a disease-free population at equilibrium. As a result, it is important for us to calculate this particular value. The basic reproduction number for our delayed Zika model given in [19] is defined as

$$
R_0 = \frac{ma^2 bce^{-\mu_v \tau}}{\mu_v(\mu_H + \gamma)}.
\tag{2.3}
$$

All the parameter values are defined as in Table 1 where b and c are the least squares estimated values obtained in R given in Table 2 corresponding to different biting rates. By substituting all the required values, we have the basic reproduction number for each biting rate shown in Table 4 to 4 d.p.

Table 4. Basic reproduction number for different biting rates.

A. *aegypti* biting rate per day	R_0
0.20	1.3176
0.50	24.7395

Note that when performing data fitting using the least squares estimation technique mentioned in Section 2.1, we notice that there are two different cases in which we can achieve a best fit against the real Zika data given by Ferguson et al. [13]. The first case is demonstrated by biting rates of $a = 0.20$ per day where the epidemic is just starting and it has yet to reach its peak epidemic level. This scenario is highlighted by having a relatively low basic reproduction number given in Table 4. Another case is when the epidemic has already reached its maximum level and this is illustrated for when $a = 0.50$ per day which has a high basic reproduction number. This is also why we noticed a huge number of recovered individuals in this case as given by (2.2). Although the basic reproduction number given when $a = 0.50$ per day is relatively high compared to the other biting rates, this value is still reasonable as various papers have also estimated a relatively high R_0 for different dengue outbreaks [20, 21].

In the next section, we will estimate the future number of cases of microcephaly due to Zika virus for different biting rates.

2.3. Estimated number of cases of microcephaly

In this section, we will focus on estimating the expected number of cases of microcephaly in Brazil due to the Zika virus both in the short-term and in the long-term. In this paper, we focus on analysing the effect of pregnant women infected with Zika virus during their first trimester as various reports (e.g. [22, 23]) suggest that pregnant women who are infected with the Zika virus during the first trimester have a much higher risk of their babies developing microcephaly as opposed to those who are infected with Zika in their second or third trimesters. This makes sense biologically as during the first trimester, the brain of the baby is still developing and thus it is more susceptible to external factors. Note that the method used in this section can be easily extended and applied to other Zika time periods and to other countries in which Zika is present.

WHO [16] state that Brazil has a total population size of 207,847,000 of which according to the United Nations [24] around 28.2% (58,612,854) were women at the age of fertility (between 15–44 years old). Recall that t_1 represents the start of 2015. The unit of time is in weeks unless stated otherwise. For the purpose of illustration, we will show only the simulations which illustrate the dynamical behaviour of humans and mosquitoes both in the long- and in the short-term in the first example.

Note that the models and parameters contain a great deal of uncertainty. We are interested in short-term estimates as they can tell us what happens in the immediate future. However we expect that in the long-term the model will settle down to a unique endemic equilibrium. Hence it is valuable to do simulations over a long time so that we can predict what will happen after the short term transient effects of the disease invading a susceptible population have faded away and we can predict the long-term consequences of Zika too.

Example 1. *(a = 0.20/day) Let us recall the estimated initial values starting from time t_1 obtained from*

parameter estimation:

$$S_H(t_1) = 207,838,200, I_H(t_1) = 314.4883, R_H(t_1) = 9,470.184,$$
$$S_v(t_1) = 311,770,600, L_v(t_1) = 308.5773, I_v(t_1) = 1,087.741$$

(2.4)

with $I_H(\eta)$ and $S_v(\eta)$ given for $\eta \in [t_1 - \tau, t_1]$ by the simulation.
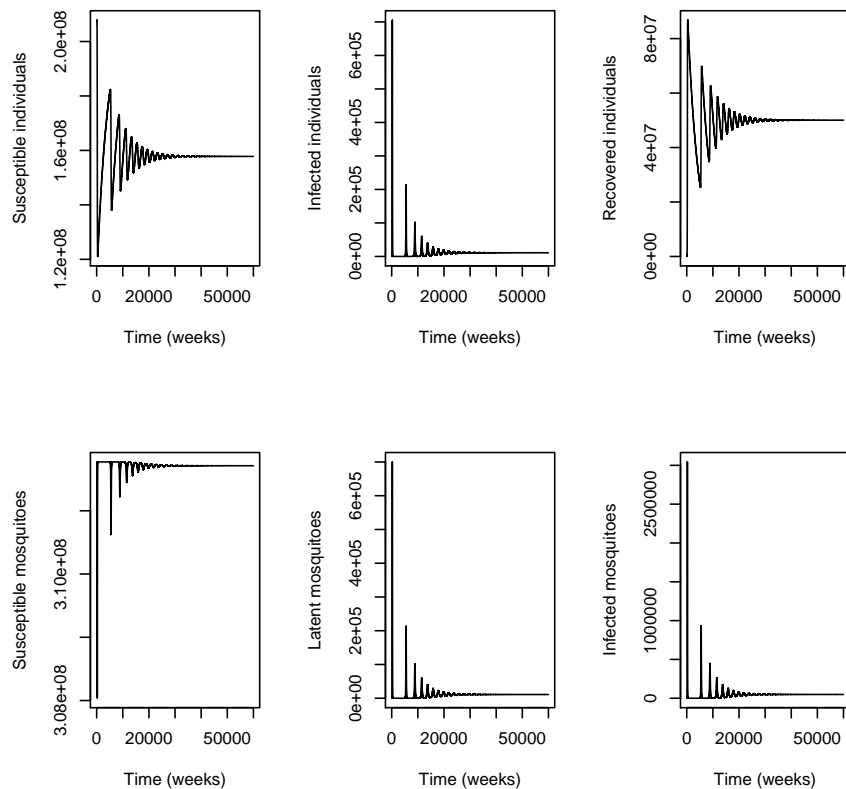
Figure 3. Numerical simulation for our solution to Eq (2.1) in the long-term using the parameter values given in Table 1 with $b = 0.2489$, $c = 0.4513$ to 4 d.p with initial values given by (2.4). The time is measured from the start of 2015.

Let us now define the parameter values as given in Table 1 but with $b = 0.2489$ and $c = 0.4513$ (to 4 d.p). Then by using R to integrate the delayed differential equations given in Eq (2.1) the numerical simulations in the long-term are as shown in Figure 3. We can see that the number of infected individuals persists with an endemic equilibrium of 10,992.89.

From various reports (e.g. [22, 23]), it is estimated that if a pregnant woman is infected with Zika during the first trimester, then the risk of her baby developing microcephaly ranges from 1% to 13%. The majority of papers in the literature estimate this probability to be in this range. However Nishiura et al. [25] estimated a higher risk of up to 100% using data from Brazil. Their estimates depend on the unknown fraction of Zika virus infections among seronegative dengue-like illness cases. Hence we also include estimates of the number of microcephaly cases when the risk of microcephaly following infection with Zika in the first trimester of preganancy is up to 100%. In order to enhance our

understanding of the effect of having different risk percentages on the number of microcephaly cases, we will produce the results where the risk percentage is 1%, 7%, 13%, 40%, 70% *and* 100%. *Note that not all of those infected pregnant women are infected during the first trimester and since pregnancy is divided into three different trimesters, we will assume that the probability that an infected pregnant woman is in the first trimester is* 1/3.

On average, each of the women currently giving birth now has been pregnant for 270 days of which the first 90 days is considered to be the first trimester in pregnancy. Recall that the average infectious period of the Zika virus is around 6 days. Let us define $M_1(t)$ to be the expected future number of cases of microcephaly in newborns as a result of pregnant women infected with the Zika virus in the first trimester. We have that M_1 is given by

$$
\begin{aligned}
M_1 &= \frac{90}{6} \frac{I^*}{N_H} \times \mu_H N_H \times P_1 \times 52 \; weeks, \\
&= 15 I^* \times \mu_H \times P_1 \times 52 \; weeks,
\end{aligned}
\tag{2.5}
$$

where P_1 represents the probability that a baby develops microcephaly given that the pregnant mother is infected in the first trimester which in this case is either 1%, 7%, 13%, 40%, 70% *or* 100%, *and* $15I^*$ *represents the number of different distinct infectious cohorts of women that will be infected during their first trimester of pregnancy. Note that I^* is the endemic equilibrium of the number of infected people which in this case is* 10,992.89. *Note also that the current model assumes that everyone in the population can give birth. If only women give birth we need to halve I^* but double μ_H which gives the same answer.*

Table 5. Expected number of microcephaly cases per year at endemic equilibrium level rounded to the nearest whole number for when $a = 0.20$/day.

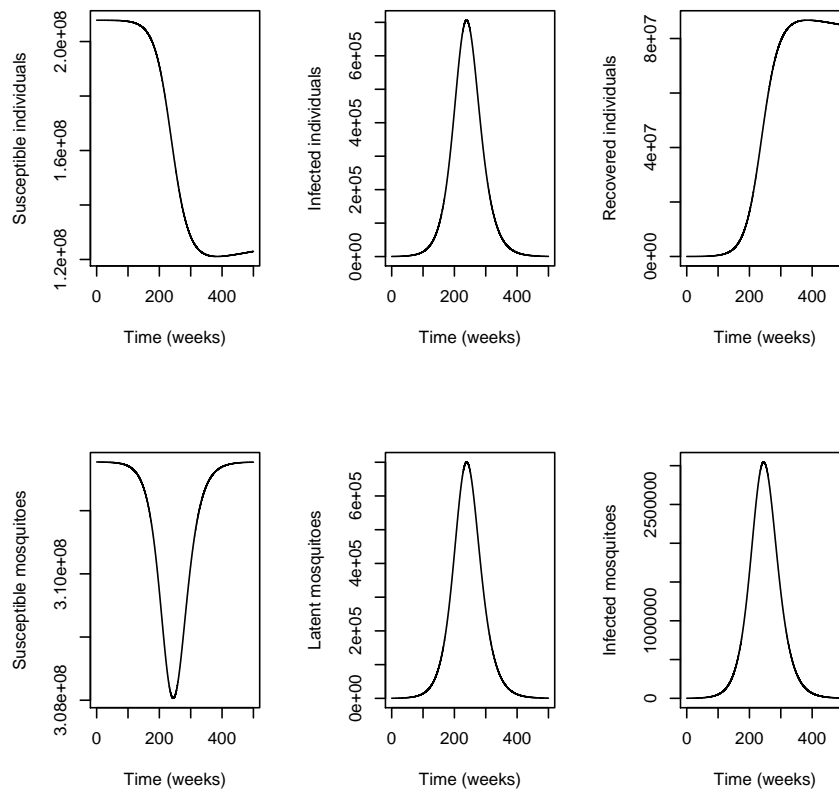| Risk percentage	Expected number of microcephaly cases per year	Risk percentage	Expected number of microcephaly cases per year
0.01	22	0.4	883
0.07	154	0.7	1,545
0.13	287	1.0	2,208

By using Eq (2.5), we can estimate the future expected number of cases of microcephaly per year in the long-term at endemic equilibrium, provided that the women are infected with the Zika virus during their first trimester of pregnancy with different risk percentages. The results are given in Table 5.

Although it is interesting for us to see the estimated number of cases of microcephaly at equilibrium, it is more practical for us to find out what happens in the short-term. As a result, we will now focus on a shorter period, say 500 weeks. For a shorter period of time, it is not suitable to use Eq (2.5) as the number of infected individuals is fluctuating over time. As a result, we will introduce an additional differential equation namely $dM(t)/dt$ which describes the number of microcephaly cases in a given time period.

$$
\frac{dM(t)}{dt} = 15 \times \mu_H I_H(t - \bar{\tau}) \times P_1,
\tag{2.6}
$$

where $\bar{\tau}$ represents the midpoint of the first trimester which in this case will be around 32.1429 weeks (to 4 d.p) and P_1 is defined as before.

Similarly, by solving Eqs (2.1) and (2.6) in R, we have the numerical simulations which illustrate the behaviour of susceptible, infected and recovered individuals over a shorter period of time, namely 500 weeks. The result is shown in Figure 4. From Figure 4, we have the numerical simulation results but in the nearer future. By integrating the differential equation $dM(t)/dt$, we have that the cumulative number of cases of microcephaly over the first 9.6 years (500 weeks) with different risk percentages are given in Table 6.

Figure 4. Numerical simulation for our solution to Eq (2.1) in the short-term using the parameter values given in Table 1 with $b = 0.2489$, $c = 0.4513$ to 4 d.p with initial values given by (2.4). The time is measured from the start of 2015.

Table 6. Expected number of microcephaly cases over the first 500 weeks rounded to the nearest whole number for when $a = 0.20$/day.

Risk percentage	Expected number of microcephaly cases	Risk percentage	Expected number of microcephaly cases
0.01	2,986	0.4	119,541
0.07	20,920	0.7	209,196
0.13	38,851	1.0	298,852

Example 2. *(a = 0.50/day) Let us recall the estimated initial values starting from time t_1 obtained from parameter estimation for when a = 0.50/day:*

$$S_H(t_1) = 6,780,497, I_H(t_1) = 2,868.188, R_H(t_1) = 201,064,600,$$
$$S_v(t_1) = 311,695,900, L_v(t_1) = 12,090.84, I_v(t_1) = 63,965.19$$

(2.7)

again the initial values for $I_H(\eta)$ and $S_v(\eta)$, $\eta \in [t_1 - \tau, t_1]$, are obtained from the simulation. By carrying out the same procedure as in Example 1, we have that the total number of infected individuals persists with an endemic equilibrium of approximately 43,818.92. The future expected number of microcephaly cases at endemic equilibrium per year caused by women who have been infected with the Zika virus in their first trimester of pregnancy with different risk percentages are given in Table 7. For over a shorter period of time, the total cumulative number of microcephaly cases over the first 9.6 years (500 weeks) with different risk percentages are given in Table 8.

Table 7. Expected number of microcephaly cases per year at endemic equilibrium level rounded to the nearest whole number for when $a = 0.50$/day.

Risk percentage	Expected number of microcephaly cases per year	Risk percentage	Expected number of microcephaly cases per year
0.01	88	0.4	3,520
0.07	616	0.7	6,160
0.13	1,144	1.0	8,800

Table 8. Expected number of microcephaly cases over the first 500 weeks rounded to the nearest whole number for when $a = 0.50$/day.

Risk percentage	Expected number of microcephaly cases	Risk percentage	Expected number of microcephaly cases
0.01	771	0.4	30,847
0.07	5,398	0.7	53,982
0.13	10,025	1.0	77,117

3. The delayed Zika model with seasonality

It is well-known that the life cycle of *A. aegypti* is influenced by many environmental factors such as rainfall and temperature (e.g. [26–28]). This might be the reason why the data fitting results shown in Figure 1 and Figure 2 are not ideal. As a result, in order to fully capture the behaviour of the *A. aegypti* under the influence of environmental factors and its effect on the number of microcephaly cases, in this section we decide to improve on our model by adding seasonality into the birth function of *A. aegypti*.

Note that the unit of time is now in weeks. Thus, our delayed Zika model with seasonality becomes:

$$
\begin{aligned}
\frac{dS_H(t)}{dt} &= -abI_v(t)\frac{S_H(t)}{N_H} - \mu_H S_H(t) + \mu_H N_H(t), \\
\frac{dI_H(t)}{dt} &= abI_v(t)\frac{S_H(t)}{N_H} - (\mu_H + \gamma)I_H(t), \\
\frac{dR_H(t)}{dt} &= \gamma I_H(t) - \mu_H R_H(t), \\
\frac{dS_v(t)}{dt} &= -acS_v(t)\frac{I_H(t)}{N_H} - \mu_v S_v(t) + \mu_v\left[1 + \alpha\sin\left(\frac{2\pi(t+\phi)}{52}\right)\right]N_v, \\
\frac{dL_v(t)}{dt} &= acS_v(t)\frac{I_H(t)}{N_H} - \mu_v L_v(t) - acS_v(t-\tau)\frac{I_H(t-\tau)}{N_H}e^{-\mu_v\tau}, \\
\frac{dI_v(t)}{dt} &= acS_v(t-\tau)\frac{I_H(t-\tau)}{N_H}e^{-\mu_v\tau} - \mu_v I_v(t),
\end{aligned}
\tag{3.1}
$$

where all the parameter values are defined as before. α is the amplitude of the seasonality function and ϕ is the peak of the function.

Because we are already fitting a large number of parameters we choose to estimate α heuristically and then fit the remaining parameters $a, b, c, t_1 - t_0$ and ϕ. Heuristically we get the best result by taking $\alpha = 1$. By choosing α to be 1 and making the same assumptions as we did in Section 2.1, we have obtained a new set of parameter values for $b, c, t_1 - t_0$ and ϕ corresponding to different biting rates which fitted the real data values for Zika in Brazil [13] much better than the ones we have obtained using Eq (2.1), which is exactly what we expected as environmental factors play an important role in the life cycle of *A. aegypti*. Recall that t_1 represents the first week of 2015 and $t_1 - t_0$ is in units of weeks. The results are shown in Table 9 with their corresponding 95% confidence intervals given in Table 10.

Similarly to before, the estimated values of $t_1 - t_0$ are the same for each value of the biting rate and the estimates for b and c for the values $a = 0.25$ per day, $a = 0.30$ per day and $a = 0.50$ per day can be obtained from the values for $a = 0.20$ per day by dividing by the corresponding ratio of a-values. So for example for $a = 0.25$ per day the values of b and c for $a = 0.20$ per day could be divided by 1.25 to obtain the new b and c values. Note also that the values of b and c for $a = 0.20$ per day, $a = 0.25$ per day, and $a = 0.30$ per day are within the range of values suggested by the literature whilst for $a = 0.50$ per day they are lower than this range of values. Because this means that all sets of different fitted values will predict the same initial values and numbers of microcephaly cases we present the results only for one of them, $a = 0.20$ per day. As before we also illustrate the results for $a = 0.5$/day with alternative least squares parameter estimates for b and c which do lie within the ranges suggested by the literature.

Table 9. Estimated values for ϕ, b, c and $t_1 - t_0$ for different biting rates to 4 d.p. ϕ and $t_1 - t_0$ are measured in weeks.

| A. *aegypti* biting rate per day	ϕ	b	c	$t_1 - t_0$
0.20	-0.2865	0.2258	0.4496	600.4457
0.50	-0.2865	0.5174	0.7168	500.4482

Table 10. 95% confidence interval for the estimated values given in Table 9 to 4 d.p.

a	ϕ	b	c	$t_1 - t_0$
0.20	$(-0.2872, -0.2858)$	$(0.2252, 0.2264)$	$(0.4484, 0.4508)$	$(599.7849, 601.1066)$
0.50	$(-0.2872, -0.2858)$	$(0.5135, 0.5214)$	$(0.7151, 0.7186)$	$(496.9703, 503.9261)$

The real Zika data in Brazil [13] from the beginning of 2015 are shown in Figure 5. The way in which we have introduced seasonality is used in many papers for mosquito-borne diseases [27, 29–34]. Over a long period of time we expect the data to follow a regular seasonal pattern. However we had only 71 weeks data available and as can be seen in Figure 5 the data has two peaks, a lower one at 17 weeks after the start of 2015 and a higher one at 6 weeks after the start of 2016. However in the output of the model with a seasonal mosquito birth rate the plotted incidence will have peaks 52 weeks apart. Additionally the design of the least squares estimation assigns equal weights to all datapoints thus it effectively gives more weight to the larger peak as there are larger potential deviations there. So even the best fit simulation is not a perfect fit to the dataset. An example fit for $a = 0.2$/day is shown in Figure 5.
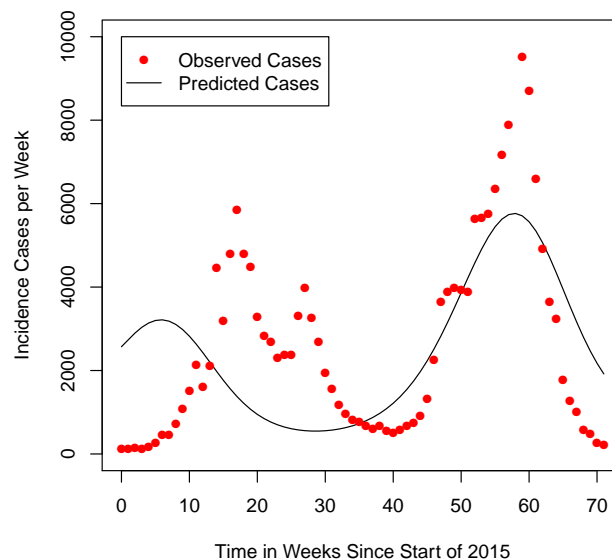
Figure 5. Numerical simulation for predicted cases of Zika obtained from Eq (3.1) plotted against the real data from Brazil from [13] with the unit of time in weeks, starting from the beginning of 2015 where $a = 0.20$/day.
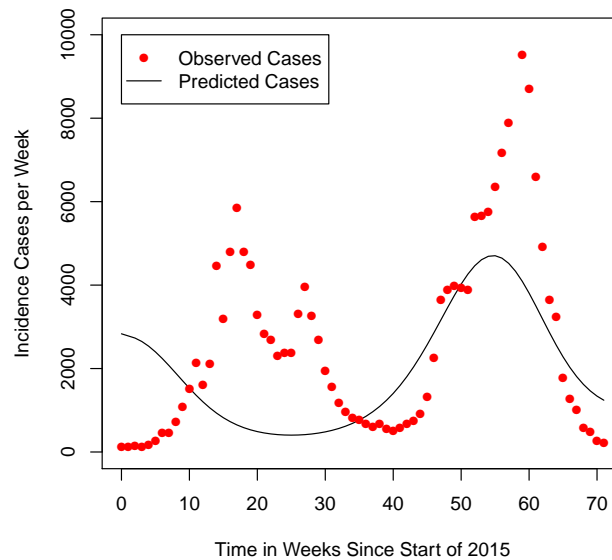
Figure 6. Numerical simulation for predicted cases of Zika obtained from Eq (3.1) plotted against the real data from Brazil from [13] with the unit of time in weeks, starting from the beginning of 2015 where $a = 0.50$/day.

The data fitting against real Zika data for each biting rate is shown in Figures 5 and 6 where the unit of time is in weeks. Note that the real Zika data in Brazil from [13] represents the incidence case data of Zika, thus in the least squares fitting to fit the output from the model we have to integrate the incidence term

$$\frac{abI_v(t)S_H(t)}{N_H},$$

equivalently $\lambda(t)S_H(t)$ where $\lambda(t) = \frac{abI_v(t)}{N_H}$ is the per capita force of infection for humans, over a week to get the incidence data for that week.

The corresponding estimated initial values in Brazil at time t_1, the first week of 2015, to 4 d.p. for each biting rate, are given as follows:

- For $a = 0.20$/day, the values at time $t_1 = t_0 + 600.4457$ weeks are

$$S_H(t_1) = 207,731,400, I_H(t_1) = 2,124.877, R_H(t_1) = 114,499.10,$$
$$S_v(t_1) = 398,139,200, L_v(t_1) = 2,692.769, I_v(t_1) = 8,371.634. \tag{3.2}$$

- For $a = 0.50$/day, the values at time $t_1 = t_0 + 595$ weeks are

$$S_H(t_1) = 7,129,476, I_H(t_1) = 2,391.525, R_H(t_1) = 200,716,100,$$
$$S_v(t_1) = 275,860,300, L_v(t_1) = 8,923.514, I_v(t_1) = 45,021.66. \tag{3.3}$$

Again in (3.2) and (3.3), the initial values for $I_H(\eta)$ and $S_v(\eta)$, $\eta \in [t_1 - \tau, t_1)$, are given by the simulation using the estimated parameter values. Similarly to Section 2.3, we will now calculate the expected number of cases of microcephaly due to Zika virus both in the short-term and at endemic equilibrium.

As the idea is similar to the ones that are presented in Section 2.3, in this section, we will illustrate the results only for when $a = 0.20$/day and for when $a = 0.50$/day, which represent the two cases we encountered in data fitting mentioned in Section 2.2.

Table 11. Expected number of microcephaly cases per year at endemic equilibrium level rounded to the nearest whole number for when $a = 0.20$/day including the effect of seasonality.

Risk percentage	Expected number of microcephaly cases per year	Risk percentage	Expected number of microcephaly cases per year
0.01	31	0.4	1,240
0.07	217	0.7	2,170
0.13	403	1.0	3,100

Example 3. *For $a = 0.20$/day, the number of infected humans has an endemic equilibrium value of around 15,417 rounded to the nearest whole number. Again by using Eq (2.5), we have that the endemic equilibrium number of cases of microcephaly per year are as given in Table 11.*

Table 12. Expected number of microcephaly cases over the first 500 weeks rounded to the nearest whole number for when $a = 0.20$/day including the effect of seasonality.

Risk percentage	Expected number of microcephaly cases	Risk percentage	Expected number of microcephaly cases
0.01	4,015	0.4	160,604
0.07	28,106	0.7	281,056
0.13	52,196	1.0	401,509

For a shorter period of time, say 600 weeks in other words in about 11.5 years, the cumulative number of microcephaly cases for the first 11.5 years caused by women being infected with the Zika virus in the first trimester of their pregnancy with different risk percentages are given in Table 12.

Table 13. Expected number of microcephaly cases per year at endemic equilibrium level rounded to the nearest whole number for when $a = 0.50$/day including the effect of seasonality.

Risk percentage	Expected number of microcephaly cases per year	Risk percentage	Expected number of microcephaly cases per year
0.01	86	0.4	3,440
0.07	602	0.7	6,020
0.13	1,118	1.0	8,600

Example 4. *For $a = 0.50$/day, the number of infected humans has an endemic equilibrium value of around 43,236 rounded to the nearest whole number. Again by using Eq (2.5), we can estimate the expected number of microcephaly cases per year in the long-term at endemic equilibrium, are as given in Table 13.*

Table 14. Expected number of microcephaly cases over the first 500 weeks rounded to the nearest whole number for when $a = 0.50$/day including the effect of seasonality.

Risk percentage	Expected number of microcephaly cases	Risk percentage	Expected number of microcephaly cases
0.01	877	0.4	35,068
0.07	6,137	0.7	61,368
0.13	11,397	1.0	87,669

For a shorter period of time, say 600 weeks in other words in about 11.5 years, the cumulative number of microcephaly cases for the first 11.5 years caused by women being infected with the Zika virus in the first trimester of their pregnancy with different risk percentages are given in Table 14.

4. Age-structured model

Another way, in which we can calculate the expected number of cases of microcephaly is to introduce the age-structure of the human population into our delayed Zika model given in Eq (2.1). Note that the unit of time is now in days for the age-structured model. Let us now define the age-structured delayed Zika model as follows:

$$
\begin{aligned}
\frac{\partial S_H(\xi,t)}{\partial t} + \frac{\partial S_H(\xi,t)}{\partial \xi} &= -abI_v(t)\frac{S_H(\xi,t)}{N_H} - \mu_H S_H(\xi,t), \\
\frac{\partial I_H(\xi,t)}{\partial t} + \frac{\partial I_H(\xi,t)}{\partial \xi} &= abI_v(t)\frac{S_H(\xi,t)}{N_H} - (\mu_H + \gamma)I_H(\xi,t), \\
\frac{\partial R_H(\xi,t)}{\partial t} + \frac{\partial R_H(\xi,t)}{\partial \xi} &= \gamma I_H(\xi,t) - \mu_H R_H(\xi,t), \\
\frac{dS_v(t)}{dt} &= -acS_v(t)\frac{\int_0^\infty I_H(\xi,t)d\xi}{N_H} - \mu_v S_v(t) + \mu_v N_v, \\
\frac{dL_v(t)}{dt} &= acS_v(t)\frac{\int_0^\infty I_H(\xi,t)d\xi}{N_H} - \mu_v L_v(t) - acS_v(t-\tau)\frac{\int_0^\infty I_H(\xi,t-\tau)d\xi}{N_H}e^{-\mu_v\tau}, \\
\frac{dI_v(t)}{dt} &= acS_v(t-\tau)\frac{\int_0^\infty I_H(\xi,t-\tau)d\xi}{N_H}e^{-\mu_v\tau} - \mu_v I_v(t),
\end{aligned}
\tag{4.1}
$$

where $S_H(0,t) = \mu_H N_H$, $R_H(0,t) = 0$ for $t \geq t_1$, $I_H(0,t) = 0$ for $t \geq t_1 - \tau$ are the boundary conditions for susceptible, recovered and infected individuals respectively. In addition, $S_H(\xi,t_1) = \mu_H N_H e^{-\mu_H\xi}$, $R_H(\xi,t_1) = 0$ and $I_H(\xi,\eta) = 0$, $\eta \in [t_1 - \tau, t_1]$, are the initial values for susceptible, recovered and infected individuals respectively. All the other parameter values and the mosquito initial conditions are defined as before. Note that $I_H(\xi,t)$ represents the density with respect to age of the number of infected individuals at time t. Therefore, the number of infected individuals between two ages, say A_1 and A_2, at time t is given as

$$
\int_{A_1}^{A_2} I_H(\xi,t)d\xi.
$$

Similarly, in order for us to calculate the future expected number of cases of microcephaly, we would introduce an additional differential equation, $dM(t)/dt$, into the Eq (4.1), and thus we have

$$
\begin{aligned}
&\frac{\partial S_H(\xi, t)}{\partial t} + \frac{\partial S_H(\xi, t)}{\partial \xi} = -abI_v(t)\frac{S_H(\xi, t)}{N_H} - \mu_H S_H(\xi, t), \\
&\frac{\partial I_H(\xi, t)}{\partial t} + \frac{\partial I_H(\xi, t)}{\partial \xi} = abI_v(t)\frac{S_H(\xi, t)}{N_H} - (\mu_H + \gamma)I_H(\xi, t), \\
&\frac{\partial R_H(\xi, t)}{\partial t} + \frac{\partial R_H(\xi, t)}{\partial \xi} = \gamma I_H(\xi, t) - \mu_H R_H(\xi, t), \\
&\frac{dS_v(t)}{dt} = -acS_v(t)\frac{\int_0^\infty I_H(\xi, t)d\xi}{N_H} - \mu_v S_v(t) + \mu_v N_v, \\
&\frac{dL_v(t)}{dt} = acS_v(t)\frac{\int_0^\infty I_H(\xi, t)d\xi}{N_H} - \mu_v L_v(t) - acS_v(t-\tau)\frac{\int_0^\infty I_H(\xi, t-\tau)d\xi}{N_H}e^{-\mu_v\tau}, \\
&\frac{dI_v(t)}{dt} = acS_v(t-\tau)\frac{\int_0^\infty I_H(\xi, t-\tau)d\xi}{N_H}e^{-\mu_v\tau} - \mu_v I_v(t), \\
&\frac{dM(t)}{dt} = 15 \times P_1\mu_H \int_0^\infty I_H(\xi, t-\bar{\tau})d\xi,
\end{aligned}
\tag{4.2}
$$

where $\bar{\tau}$ and P_1 are defined as before.

Example 5. *(a = 0.20/day) By using the parameter estimated values b, c and $t_1 - t_0$ from Section 2.1 and other parameter values given in Table 1 with a = 0.20/day, we have obtained that for the next 800 days (around 2.19 years), the cumulative number of microcephaly cases is estimated to be around 595, 4,165 and 7,735 (to the nearest whole number) corresponding to having risk percentage of 1%, 7% and 13% respectively. For risk percentages 40%, 70% and 100% these numbers are 23,800, 41,650 and 59,500 respectively.*

Example 6. *(a = 0.50/day) By using the parameter estimated values b, c and $t_1 - t_0$ from Section 2.1 and other parameter values given in Table 1 with a = 0.50/day, we have obtained that for the next 800 days (around 2.19 years), the cumulative number of microcephaly cases is estimated to be around 162, 1,135 and 2,106 (to the nearest whole number) corresponding to having risk percentage of 1%, 7% and 13% respectively. For risk percentages 40%, 70% and 100% these numbers become respectively 6,480, 11,340 and 16,200.*

Note that the computational time required to generate the results for this age-structured model is considerably longer than for the model given in Eq (2.1) and thus it is difficult to produce results for a longer period of time.

5. The delayed age-structured Zika model with seasonality

In this section, we will continue to examine the effect of seasonality on the spread of the Zika virus by now introducing seasonality into the more complicated age-structured Zika model. As before, we would also need to introduce an additional differential equation $dM(t)/dt$ which will allow us to calculate the expected future number of cases of microcephaly at a particular time period. Note that

the unit of time is now in days for the age-structured model. Thus we have

$$\frac{\partial S_H(\xi,t)}{\partial t} + \frac{\partial S_H(\xi,t)}{\partial \xi} = -abI_v(t)\frac{S_H(\xi,t)}{N_H} - \mu_H S_H(\xi,t),$$

$$\frac{\partial I_H(\xi,t)}{\partial t} + \frac{\partial I_H(\xi,t)}{\partial \xi} = abI_v(t)\frac{S_H(\xi,t)}{N_H} - (\mu_H + \gamma)I_H(\xi,t),$$

$$\frac{\partial R_H(\xi,t)}{\partial t} + \frac{\partial R_H(\xi,t)}{\partial \xi} = \gamma I_H(\xi,t) - \mu_H R_H(\xi,t),$$

$$\frac{dS_v(t)}{dt} = -acS_v(t)\frac{\int_0^\infty I_H(\xi,t)d\xi}{N_H} - \mu_v S_v(t) + \mu_v\left[1 + \alpha\sin\left(\frac{2\pi(t+\phi)}{365}\right)\right]N_v, \qquad (5.1)$$

$$\frac{dL_v(t)}{dt} = acS_v(t)\frac{\int_0^\infty I_H(\xi,t)d\xi}{N_H} - \mu_v L_v(t) - acS_v(t-\tau)\frac{\int_0^\infty I_H(\xi,t-\tau)d\xi}{N_H}e^{-\mu_v\tau},$$

$$\frac{dI_v(t)}{dt} = acS_v(t-\tau)\frac{\int_0^\infty I_H(\xi,t-\tau)d\xi}{N_H}e^{-\mu_v\tau} - \mu_v I_v(t),$$

$$\frac{dM(t)}{dt} = 15 \times P_1\mu_H\int_0^\infty I_H(\xi,t-\bar{\tau})d\xi,$$

where $\bar{\tau}$ and P_1 are defined as before.

Example 7. *(a = 0.20/day) Let us recall that for a = 0.20/day, in the non-age-structured seasonal model, $\alpha = 1$ and $\phi = -0.2865$ weeks. By solving the differential equations, including $dM(t)/dt$, we have that in the next 900 days (around 2.47 years), the cumulative number of cases of microcephaly is around 702, 4,914 and 9,126 (to the nearest whole number) corresponding to having risk percentage of 1%, 7% and 13% respectively. For risk percentages 40%, 70% and 100% these numbers are 28,080, 49,140 and 70,200 respectively.*

Example 8. *(a = 0.50/day) Again recall that for a = 0.5/day, in the non-age-structured seasonal model, $\alpha = 1$ and $\phi = -0.2865$ weeks. Similarly, by solving the differential equations, including $dM(t)/dt$, we have that in the next 900 days (around 2.47 years), the cumulative number of cases of microcephaly is around 189, 1,323 and 2,457 (to the nearest whole number) corresponding to having risk percentage of 1%, 7% and 13% respectively. For risk percentages 40%, 70% and 100% these numbers become respectively 7,560, 13,230 and 18,900.*

Again due to the computational time required to generate the results for this age-structured model being considerably longer than for the model given in Eq (3.1) it is difficult to produce results for a longer period of time.

6. Conclusion and discussion

Zika virus is transmitted by *A. aegypti*, the same mosquitoes that are responsible for the transmission of dengue. Although the Zika virus has been around for a while, it has not received much attention until now, when the connection between the Zika virus and microcephaly has recently been discovered. Microcephaly is a serious birth defect in newborns. Motivated by this, in this paper, we focused on using mathematical models and numerical simulations to calculate the future expected number of cases of microcephaly if pregnant women are exposed to Zika.

We used four different approaches to examine this. The first one is using an existing delayed dengue model mentioned in [1], the second one is introducing the age-structure of the human population. The third one is introducing seasonality into the birth function of the *A. aegypti* mosquitoes to monitor the effect that environmental factors such as rainfall and temperature would have on the spread of Zika between humans and mosquitoes. Lastly, we continue to investigate the effect of seasonality but now on the more complicated age-structured model.

We have used the least squares estimation technique to estimate the two crucial parameter values namely the transmission probabilities between humans and *A. aegypti*. We have also calculated the basic reproduction number which is a threshold that determines whether a disease will die out or persist over time. We have fitted our models against real Zika data in Brazil from Ferguson et al. [13]. The data fitting results for our seasonality model are as given in Figures 5–6. The method by which we incorporate the effect of seasonality into our model is a well-known method used in many papers (e.g. [27,29–34]). The estimated transmission probabilities obtained for Zika between *A. aegypti* mosquitoes and humans are within the ranges given by the literature.

For each approach, we then solve the ODEs and PDEs using the programming language R and produced results in the long- and short-term which will help us with future planning and control policies for Zika in relation to microcephaly. We have introduced an additional differential equation $dM(t)/dt$ into our model where $M(t)$ represents the total cumulative expected future number of cases of microcephaly from the start up to a given time. Numerical simulations are then produced throughout the paper to give our results. Note that the techniques we used in this paper can be applied to any countries that have Zika or even other mosquito-born diseases such as dengue, yellow fever and chikungunya which are all spread by *A. aegypti* mosquitoes or other mosquito-born diseases, for example malaria.

In Sections 4 and 5, we focussed on the age-structured Zika model with and without seasonality respectively. In both cases we have used the differential equation

$$\frac{dM(t)}{dt} = 15\mu_H \int_0^\infty I_H(\xi, t - \bar{\tau})d\xi \times P_1, \tag{6.1}$$

where $\bar{\tau}$ is the time from the midpoint of the first trimester to birth. This is based on the observation that the average duration of infection is 6 days and the first trimester of pregnancy lasts 90 days. So assuming as a simplification that each infection lasts exactly 6 days and the level of infection during the first trimester of individuals giving birth now was approximately constant at the midpoint of that 6-day interval a slightly more accurate but more complex version is given by

$$\frac{dM(t)}{dt} = \mu_H \Big(\int_0^\infty I_H(\xi, t - \bar{\tau}_1)d\xi + \int_0^\infty I_H(\xi, t - \bar{\tau}_2)d\xi \tag{6.2}$$
$$+ \int_0^\infty I_H(\xi, t - \bar{\tau}_3)d\xi + \cdots + \int_0^\infty I_H(\xi, t - \bar{\tau}_{15})d\xi \Big) P_1,$$

where $\bar{\tau}_1$ is three days into the first trimester, the midpoint of the first infectious period of pregnancy, $\bar{\tau}_2$ is nine days into the first trimester, $\bar{\tau}_3$ is fifteen days into the first trimester … and so on up to $\bar{\tau}_{15}$ which is three days before the end of the first trimester.

However if the age-related fertility rate for Brazil is available then we can use an alternative approach in working out the expected number of cases of microcephaly. To be more specific the new

differential equation for $\frac{dM(t)}{dt}$ will become

$$\frac{dM(t)}{dt} = \frac{15}{2} \int_0^\infty I_H(\xi, t - \bar{\tau}) f(\xi, t - \tau_1) d\xi \times P_1. \tag{6.3}$$

Here $f(\xi, t)$ represents the age-related fertility rates for different age-groups in Brazil, τ_1 is 270 days which is the average length of a pregnancy and $\bar{\tau}$ is 225 days which is the average length of time from the midpoint of the first trimester to delivery. P_1 is defined as before. Equation (6.3) is derived from Eq (6.1) by introducing the age-dependent fertility rate and dividing by two as only females reproduce. However if we decide to use this approach then the population size will vary with respect to time and thus we would also need to use age-related birth and death rates. As a result the age-structured model would become significantly more complicated.

As before we can make this model more accurate by dividing the first trimester up into fifteen distinct six day periods and using the midpoint of each instead of a single approximation at the midpoint of the first trimester to give

$$\frac{dM(t)}{dt} = \frac{1}{2} \Big(\int_0^\infty I_H(\xi, t - \bar{\tau}_1) f(\xi, t - \tau_1) d\xi + \int_0^\infty I_H(\xi, t - \bar{\tau}_2) f(\xi, t - \tau_1) d\xi \tag{6.4}$$
$$+ \int_0^\infty I_H(\xi, t - \bar{\tau}_3) f(\xi, t - \tau_1) d\xi + \cdots + \int_0^\infty I_H(\xi, t - \bar{\tau}_{15}) f(\xi, t - \tau_1) d\xi \Big) P_1.$$

The first Zika case was first reported in Brazil in 2015. Since then there has been a rapid increase in the number of Zika cases all across the country. According to the report given by [35], the number of Zika cases in Brazil reached its peak in Week 6 of 2016 with around 17,800 suspected cases of which around 11,000 of them were confirmed. From the report given in [35], between 2016 and 2017, various states in the central-West region of Brazil have recorded high Zika incidence rates as shown in Table 15.

Table 15. Zika incidence rates in States of Brazil [35].

States in Brazil	Zika incidence rate (per 100,000)
Mato Grosso	663
Rio de Janeiro	412
Bahia	339
Alagoas	205
Goias	154

For the purposes of comparison of the figures obtained in this paper with actual data, at April 23, 2016, the number of confirmed and suspected cases of microcephaly was 4,908, just one case more than a week earlier. Of these the number of confirmed cases climbed to 1,198 from 1,168 a week earlier. Brazil had registered 91,387 likely cases of Zika infection in the period February until April 2, 2016 with the most diagnoses in Rio de Janeiro [36]. In addition from another report [37], for the period between August 2015 up to June 25th, 2016, there were 8,165 notified microcephaly cases in Brazil of which 1,638 were confirmed, 3,466 excluded and 3,061 under investigation.

We may ask which of our four models performs the best. We know that for other mosquito-borne diseases the mosquito population varies according to the time of year. Additionally by comparing the

data fitting results from the Zika model against the results from the Zika model with seasonality, the ones with seasonality provide a better fit against the real Zika data in Brazil. Moreover as fertility rates vary with age we expect the age-structured models to be more accurate. Hence in general the age-structured seasonal model should give the best answer. Note that as we had data only for a relatively short timescale it was difficult to estimate parameters for the seasonal models. Also the age-structured models could predict the short-term incidence of microcephaly but because of the computing power needed they could not predict long-term endemic levels of microcephaly cases. Thus all of the models have different advantages and disadvantages.

One of the motivations behind this paper is the recent discovery of the connection between the Zika virus and microcephaly and other birth defects in newborns. It is important for us to understand how many of the microcephaly cases are directly caused by pregnant women being exposed to Zika and thus its impact on pregnant women travelling to countries infected with the Zika virus. Therefore, we have obtained simulations which allow us to calculate the expected future number of cases of microcephaly as a result of women being pregnant and thus infected with Zika during their first trimester of pregnancy. Furthermore, the technique used here can be applied to analysing the association between the Zika virus and other birth defects such as Guillain-Barré Syndrome. These results will be beneficial for policy makers in deciding the risk involved for pregnant women travelling to countries infected with Zika.

The models discussed in this paper assume that the transmission of Zika in Brazil occurs in a homogeneous fashion within a single population. Of course this assumption is not realistic as Brazil has a huge human population distributed over a large area. Thus transmission parameters will in practice vary throughout the country. Moreover climatic conditions and socio-economic variables such as urban or rural settings vary greatly through the country causing different population dynamics for vector populations. Therefore using a single parameter for mosquito populations may not be realistic even if assuming an average value. So ideally we should break down the population into smaller regions and use different parameters for each region. However such data are difficult to find.

In addition epidemic models commonly assume a homogeneously mixing population as an approximation. For example Agusto et al. [38] model malaria transmission using a host-vector model in different regions of Africa using a geographically homogeneous model. Some of the parameters are temperature dependent but there is no other spatial geographical variability. Koutou et al. [39] apply a homogeneous host-vector model for malaria transmission to model vector population growth and malaria virus transmission to humans. Coudeville and Garnett [40] applied a geographically heterogeneous host-vector model to estimate the potential impact of dengue vaccination in South Vietnam. Maier et al. [41] used a spatially geographically heterogeneous host-vector model to analyse the effect of the Sanofi Pasteur vaccine Dengvaxia in Brazil. Gao et al. [42] discuss a homogeneously mixing compartmental model for the transmission of Zika and apply it to data in Brazil, Colombia and El Salvador. This applies the same model parameters to the three countries and their model provides good fits to the observed data. Wang et al. [43] discuss modelling and control of Zika in Brazil using the *Wolbachia* parasite. They also use a spatially geographically homogeneous model.

Amaku et al. [44, 45] deploy a similar geographically homogeneous disease transmission model to estimate the prevalence of undiagnosed hepatitis C virus (HCV) infections across the whole of Brazil. Similarly to Zika the actual disease transmission parameters, for example needle sharing rates for HCV, will vary throughout Brazil, but a spatially homogeneous model is used as an approximation.

The models discussed in this paper consider only transmission of Zika between humans and mosquitoes. Other potential transmission routes such as sexual transmission and vertical transmission from an infected human mother to her child have not been included. Vertical transmission of Zika can occur but is thought to be rare. Recent studies have shown that although sexual transmission of Zika can occur this is a very small component of disease transmission and also recent evidence suggests that the risk of sexual transmission of Zika may dissipate quickly [46, 47]. There is also a good deal of uncertainty about the effect of sexual transmission [48].

Several previous models have been developed to model the spread of the Zika virus. Kucharski et al. [49] study a mathematical model for the 2013–2014 French Polynesia outbreak. This model focusses on human vector transmission which it says is the main transmission method. Funk et al. [50] compares three outbreaks of dengue and Zika virus in two different island settings in Micronesia, the Yap main island and Fais using a mathematical model. Again they focus on host-vector transmission and ignore the effects of sexual transmission.

Majumder et al. [51] also say that Zika virus is primarily transmitted by *Aedes* mosquitoes although evidence of vertical human to human and sexual transmission between humans exists. The basic reproduction number was estimated from data.

In their model Gao et al. [42] also include sexual transmission of Zika. They find that it plays a small part in Zika transmission, contributing about 3.04% to the R_0 value and 4.44% of the total transmission attack rate, although the confidence intervals for these percentages are quite large. Sexual transmission seems to be modelled crudely as a disease spread by direct contact rather than by dividing the population into males and females. Wang et al. [43] develop a model for using the *Wolbachia* bacteria to control Zika. They include sexual transmission between humans but again model it crudely as a disease spread by direct contact. Moreover again from their estimated parameter values it seems as though the effect of sexual transmission is small compared with the route between humans and vectors.

Hence although human to human vertical and sexual transmission of Zika exist their effect is small compared with spread between humans and mosquitoes and also computationally difficult to model accurately as this would increase the model complexity. Therefore we follow Kucharski et al. [49] and Funk et al. [50] and do not explicitly include either vertical or sexual human transmission in our model.

Acknowledgements

Conflict of interest

All authors declare no conflicts of interest in this paper.

References

1. E. Massad, F. A. B. Coutinho, M. N. Burattini, et al., Estimation of R_0 from the initial phase of an outbreak of a vector-borne infection, *Trop. Med. Int. Health*, **15** (2010), 120–126.

2. G. Adamu, M. Bawa, M. Jiya, et al., A mathematical model for the dynamics of Zika virus via homotopy perturbation method, *J. Appl. Sci. Environ. Manage.*, **21** (2017), 615–623.

3. E. Bonyah and K. O. Okosun, Mathematical modeling of Zika virus, *Asian Pac. J. Trop. Dis.*, **6** (2016), 673–679.

4. C. Ding, N. Tao and Y. Zhu, A mathematical model of Zika virus and its optimal control, *In Proc. of the 35th CCC Conf., 2016, Chengdu, China*, (2016), 2642–2645.

5. G. González-Parra and T. Benincasa, Mathematical modeling and numerical simulations of Zika in Colombia considering mutation, *Math. Comput. Simul.*, **163** (2019), 1–8.

6. N. K. Goswami, A. K. Srivastav, M. Ghosh, et al., Mathematical modeling of Zika virus disease with nonlinear incidence and optimal control, in *J. Phys. Conf. Ser.*, **1000** (2018), 1–16.

7. B. Mahatoa and B. K. Mishrab, Global stability analysis on the transmission dynamics of Zika virus, *Int. J. Appl. Eng. Res.*, **13** (2018), 12296–12303.

8. S. C. Mpeshe, N. Nyerere and S. Sanga, Modeling approach to investigate the dynamics of Zika virus fever: a neglected disease in Africa, *Int. J. Adv. Appl. Math. Mech.* **4** (2017), 14–21.

9. F. Ndairou, I. Area, J. J. Nieto, et al., Mathematical modeling of Zika disease in pregnant women and newborns with microcephaly in Brazil, *Math. Meth. Appl. Sci.* **41** (2018), 8929–8941.

10. T. O. Oluyo and M. O. Adeyemi, Mathematical analysis of Zika epidemic model, *IOSR J. Math.*, **12** (2016), 21–33.

11. B. Tang, Y. Xiao and J. Wu, Implication of vaccination against dengue for Zika outbreak, *Sci. Rep.*, **6** (2016), article number 35623.

12. B. Tang, W. Zhou, Y. Xiao, et al., Implication of sexual transmission of Zika on dengue and Zika outbreaks, *Math. Biosci. Eng.*, **16** (2019), 5092–5113.

13. N. M. Ferguson, Z. M. Cucunubá, I. Dorigatti, et al., Countering the Zika epidemic in Latin America, *Science*, **353** (2016), 353–354.

14. M. Andraud, N. Hens, C. Marais, et al., Dynamic epidemiological models for dengue transmission: a systematic review of structural approaches, *PLoS One*, **7** (2012), p.e49085.

15. E. Chikak and H. Ishikawa, A dengue transmission model in Thailand considering sequential infections with all four serotypes, *J. Infect. Dev. Countr.*, **3** (2009), 711–722.

16. *World Health Organization. Countries: Brazil*, 2017. Available from: `http://www.who.int/countries/bra/en/`.

17. *Centers for Disease Control and Prevention*, Surveillance and control of *Aedes aegypti* and *Aedes albopictus* in the United States, 2017. Available from: `https://www.cdc.gov/chikungunya/resources/vector-control.html`.

18. D. Focks, N. Alexander and E. Villegas, Multicountry study of *Aedes aegypti* pupal productivity survey methodology: findings and recommendations, *UNICEF/UNDP/World Bank/WHO Special*

Programme for Research and Training in Tropical Disease (TDR), 2006. Available from: `http://www.who.int/tdr/publications/documents/aedes_aegypti.pdf`.

19. E. Massad, F. A. B. Coutinho, M. N. Burattini, et al., The risk of yellow fever in a dengue-infested area, *Trans. R. Soc. Trop. Med. Hyg.*, **95** (2001), 370–374.

20. G. Chowell, R. Fuentes, A. Olea, et al., The basic reproduction number R_0 and effectiveness of reactive interventions during dengue epidemics: The 2002 dengue outbreak in Easter Island, Chile, *Math. Biosci. Eng.*, **10** (2013), 1455–1474.

21. A. K. Supriatna, Estimating the basic reproduction number of dengue transmission during 2002-2007 outbreaks in Bandung, Indonesia, *WHO Regional Office for South-East Asia. Dengue Bulletin*, **33** (2009), 21–33. Available from: `http://www.who.int/iris/handle/10665/170937`.

22. S. Cauchemez, M. Besnard, P. Bompard, et al., Association between Zika virus and microcephaly in French Polynesia, 2013-2015: a retrospective study, *The Lancet*, **387** (2016), 2125–2132.

23. M. A. Johansson, L. Mier-y-Teran-Romero, J. Reefhuis, et al., Zika and the risk of of microcephaly, *N. Engl. J. Med.*, **375** (2016), 1–4.

24. *United Nations*, United Nations, department of economic and social affairs, population division. World population prospects: The 2015 revision, (2015). Available from: `https://esa.un.org/unpd/wpp/Graphs/DemographicProfiles/`.

25. H. Nishiura, K. Mizumoto, K. S. Rock, et al., A theoretical estimate of the risk of microcephaly during pregnancy, *Epidemics*, **15** (2016), 66–70.

26. J. Liu-Helmersson, H. Stenlund, A. Wilder-Smith, et al., Vectorial capacity of *Aedes aegypti*: effects of temperature and implications for global dengue epidemic potential, *PLoS One*, **9** (2014), e89783.

27. H. S. Rodrigues, M. T. Monteiro and D. M. Torres, Seasonality effects on dengue: basic reproduction number, sensitivity analysis and optimal control, *Math. Meth. Appl. Sci.*, **39** (2016), 4671–4679.

28. S. Wiwanitkit and V. Wiwanitkit, Predicted pattern of Zika virus infection distribution with reference to rainfall in Thailand, *Asian Pac. J. Trop. Med.*, **9** (2016), 719–720.

29. A. G. Barnett, P. Baker and A. J. Dobson, Analysing seasonal data, *The R Journal*, **4** (2012). Available from: `https://journal.r-project.org/archive/2012/RJ-2012-001/RJ-2012-001.pdf`.

30. M. N. Burattini, M. Chen, A. Chow, et al., Modelling the control strategies against dengue in Singapore, *Epidemiol. Infect.*, **136** (2008), 309–319.

31. N. M. Ferguson, Z. M. Cucunubá, I. Dorigatti, et al., Supplementary materials for countering the Zika epidemic in Latin America, 2016. Available from: `www.sciencemag.org/content/353/6297/353/suppl/DC1`.

32. E. Massad, F. A. B. Coutinho, L. F. Lopez, et al., Modelling the impact of global warming on vector-borne infections, *Phys. Life Rev.*, **8** (2011), 169–199.

33. H. S. Rodrigues, M. T. Monteiro and D. M. Torres, Seasonality effects on dengue, *In Proc. of the 14th CMMSE Conf. Costa Ballena, Rota, Cadiz, Spain, 2014*, (2014), 1084–1091.

34. A. M. Stolwijk, H. Straatman and G. A. Zielhuis, Studying seasonality by using sine and cosine functions in regression analysis, *J. Epidemiol. Commun. Health*, **53** (1999), 235–238.

35. *Pan American Health Organization/World Heath Organization*, Zika-epidemiological report Brazil. Washington, D.C: PAHO/WHO, 2017.

36. B. Haynes and A. Boadle, Brazil says Zika-linked microcephaly cases stable at 4,908, *Health News*, 2016. Available from `http://www.reuters.com/article/us-health-zika-brazil-idUSKCN0XN2NP`.

37. T. V. de Araújo, L. C. Rodrigues, R. A. de Alencar Ximenes, et al., Association between Zika virus infection and microcephaly in Brazil, January to May, 2016: preliminary report of a case-control study, *The Lancet Infect. Dis.*, **16** (2016), 1356–1363.

38. F. B. Agusto, A. B. Gumel and P. E. Parham, Qualitative assessment of the role of temperature variations in malaria transmission dynamics, *J. Biol. Syst.*, **23** (2015), 597–630.

39. O. Koutou, B. Traoré and B. Sangoré, Mathematical modelling of malaria transmission global dynamics taking into account the immature stages of the vectors, *Adv. in Differ. Equ.*, **2018**, 220.

40. L. Coudeville and G. P. Garnett, Transmission dynamics of the four dengue serotypes in Southern Vietnam and the potential impact of vaccination, *PLoS One*, **7** (2012), e51244.

41. S. B. Maier, X. Huang, E. Massad, et al., Analysis of the optimal age for dengue vaccination in Brazil with a tetravalent dengue vaccine, *Math. Biosci.*, **294** (2017), 15–32.

42. D. Gao, Y. Lou, D. He, et al., Prevention and control of Zika as a mosquito-borne and sexually transmitted disease: a mathematical modeling analysis, *Sci. Rep.*, **6** (2016), Article Number 28070.

43. L. Wang, H. Zhao, S. M. Oliva, et al., Modelling the transmission and control of Zika in Brazil, *Sci. Rep.*, **7** (2017), article number 7721.

44. M. Amaku, M. N. Burattini, F. A. B. Coutinho, et al., Estimating the size of the HCV infection prevalence: a modelling approach using the incidence of cases reported to an official notification system, *Bull. Math. Biol.*, **78** (2016), 970–990.

45. M. Amaku, M. N. Burattini, E. Chaib, et al., Estimating the prevalence of infectious diseases from under-reported age-dependent compulsorily notification databases, *Theor. Biol. Med. Model.*, **14** (2017), 23.

46. P. S. Mead, N. K. Duggal, S. A. Hook, et al., Zika virus shedding in semen of symptomatic infected men, *N. Engl. J. Med.*, **378** (2018), 1377–1385.

47. M. Zamani and V. Zamani, Sexual transmission of Zika virus: an assessment of the evidence, *Iran. J. Public Health*, **46** (2017), 1305–1306.

48. R. Lowe, C. Barcellos, P. Brasil, et al., The Zika virus epidemic in Brazil: from discovery to future implications, *Int. J. Environ. Res. Public Health*, **15** (2018), E96.

49. A. J. Kucharski, S. Funk, R. M. Eggo, et al., Transmission dynamics of Zika virus in island populations: a modelling analysis of the 2013-14 French Polynesia outbreak, *PLoS Negl. Trop. Dis.*, **10** (2016), e0004726.

50. S. Funk, A. J. Kucharski, A. Camacho, et al., Comparative analysis of dengue and Zika outbreaks reveals differences by setting and virus, *PLoS Negl. Trop. Dis.*, **10** (2016), e0005173.

51. M. S. Majumder, M. Santillana, S. R. Mekaru, et al., Utilizing nontraditional data sources for real-time estimation of transmission dynamics during the 2015-2016 Colombian Zika virus disease outbreak, *JMIR Public Health Surveill.*, **2** (2016), e30.

AIMS Press